

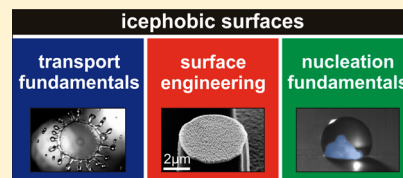
# Physics of Icing and Rational Design of Surfaces with Extraordinary Icephobicity

Thomas M. Schutzius, Stefan Jung, Tanmoy Maitra, Patric Eberle, Carlo Antonini, Christos Stamatopoulos, and Dimos Poulikakos\*

Laboratory of Thermodynamics in Emerging Technologies, Mechanical and Process Engineering Department, ETH Zurich, 8092 Zurich, Switzerland

## S Supporting Information

**ABSTRACT:** Icing of surfaces is commonplace in nature and technology, affecting everyday life and sometimes causing catastrophic events. Understanding (and counteracting) surface icing brings with it significant scientific challenges that requires interdisciplinary knowledge from diverse scientific fields such as nucleation thermodynamics and heat transfer, fluid dynamics, surface chemistry, and surface nanoengineering. Here we discuss key aspects and findings related to the physics of ice formation on surfaces and show how such knowledge could be employed to rationally develop surfaces with extreme resistance to icing (extraordinary icephobicity). Although superhydrophobic surfaces with micro-, nano-, or (often biomimetic) hierarchical roughnesses have shown in laboratory settings (under certain conditions) excellent repellency and low adhesion to water down to temperatures near or below the freezing point, extreme icephobicity necessitates additional important functionalities. Other approaches, such as lubricant-impregnated surfaces, exhibit both advantages and serious limitations with respect to icing. In all, a clear path toward passive surfaces with extreme resistance to ice formation remains a challenge, but it is one well worth undertaking. Equally important to potential applications is scalable surface manufacturing and the ability of icephobic surfaces to perform reliably and sustainably outside the laboratory under adverse conditions. Surfaces should possess mechanical and chemical stability, and they should be thermally resilient. Such issues and related research directions are also addressed in this article.



## 1. INTRODUCTION

Because of its ubiquitous nature and the serious safety, production, and performance issues it poses, ice formation is a research topic that has received considerable attention. In recent years, as a result of the emergence of methods of surface nanoengineering and the (related) vivid interest of the research community on the topic of superhydrophobicity, the goal of developing surfaces with extraordinary resistance to ice formation and retention is taking center stage in the activities of many researchers, bringing with it a host of additional challenges. One could loosely use the term supericephobicity for such surfaces but with the qualifier that no consensus for a quantifiable definition of this term exists in the literature so far.

Many aspects of icing remain poorly understood and are therefore difficult to predict because of the relative complexity of the problem. It is a multiphase process, which is highly sensitive to environmental conditions, and it is based on water, which has unique physical properties and complex behavior. These are important points because any serious attempt to generate an icephobic (ice-repellent) surface is based on the premise that a good understanding of its underlying mechanisms is in place or needs to be attained first. Thermodynamically, there are three pathways to ice formation: (1) vapor–solid, (2) vapor–liquid–solid, and (3) liquid–solid. In general, because of the different nucleation and growth mechanisms associated with each of these phase-transformation processes,<sup>1</sup> a unifying surface that is able to address all of these simultaneously and inhibits ice formation

passively appears to be far from reality. Hence, from an engineering perspective, if one poses the broad question of what constitutes a truly icephobic surface, then one must often respond that it depends, because the environmental and operating conditions affect ice formation greatly and therefore the design of icephobic surfaces.

With these perspectives in mind, the following article provides an overview and vision of how the authors and other researchers working on similar topics rationalize their approach to icephobicity. From a knowledge dissemination perspective, icephobicity is becoming a research topic with a rapidly increasing presence and impact annually, as defined by citations (Figure 1), and has broad commercial appeal; however, its success from an application perspective has been limited. Because of their relevance to industrial/commercial applications, this article mainly discusses liquid–solid and vapor–liquid–solid transition pathways to ice formation, which are of great importance to icing in nature and many engineering applications. For these transition types, we considered studies in which different environmental conditions, surface geometry, and surface wettability (intrinsic) were investigated in order to elucidate the nuances of the icing process and therefore guide the design of high-performance supericephobic surfaces. This

Received: July 2, 2014

Revised: October 21, 2014

Published: October 25, 2014

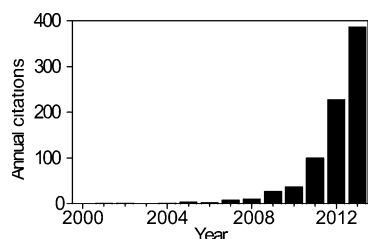


**Figure 1.** Number of citations by year for the following topics: icephobic or anti-icing (excluding patents and review papers). Searches done on Web of Science.

approach necessitates a fusion of fluid mechanics (droplet transport and related droplet/surface interactions) and thermodynamics (nucleation theory and heat transfer) in order to rationalize surface engineering. Because there are already many reports on anti-icing surfaces (reviews, experimental, and theoretical papers), it is necessary to place this one in context. Although a previous review and work emphasized biology as a guiding principle for surface construction<sup>2</sup> or focused solely on the capabilities of superhydrophobic surfaces as a strategy,<sup>3</sup> this review aims to outline a series of works utilizing design principles based upon thermodynamics and fluid mechanics that focused on eliminating the formation of ice on a surface under atmospheric conditions, which stands in contrast to works that emphasize reducing ice adhesion once ice has formed. We begin by considering aspects of nucleation theory and heat transfer, and then we move on to the transport of droplets in a metastable liquid phase (supercooled). We subsequently combine and utilize these two perspectives to rationalize the construction of engineered icephobic surfaces. We give due consideration to the need for long-term performance (also under adverse conditions) and the scalability of a given fabrication process because industrial implementation is generally the final, long-term goal of these efforts. With all of this, we give some final thoughts to where we think the research is headed and the big problems to surmount.

## 2. ICE NUCLEATION CONSIDERATIONS: TOWARD RATIONAL ICEPHOBIC SURFACE DESIGN

The first step in the rational design of surfaces that inhibit ice formation is to gain a substantial understanding of ice nucleation, because it is the origin of phase transformation in nature and technology. To facilitate the discussion, Figure 2 shows a

schematic representation of the relevant effects and parameters used to describe the ice nucleation physics. Figure 2a shows the condition required for homogeneous nucleation to proceed, which is depicted in the classic plot of the change in Gibbs free energy ( $\Delta G$ ) versus ice embryo radius ( $r$ ). Figure 2b shows spatially where nucleation can occur within a liquid droplet: at the free interface (homogeneous nucleation) or at the solid interface (heterogeneous). Figure 2c shows how surface curvature can affect the formation of a critical ice embryo (increasing the ice–water contact angle).

Strategies to prevent ice formation and therefore ice nucleation on surface structures have been studied since the 1950s.<sup>4</sup> If we look to nature for inspiration, then we see that biological organisms have adopted a number of strategies to survive cold climate conditions, including the so-called antifreeze protein (AFP).<sup>5</sup> AFPs in fish living in polar climates can depress body fluid freezing down to  $-2$  °C, and AFPs in insects can prevent freezing down to temperatures of as low as  $-10$  °C.<sup>5</sup> The antifreezing character of AFPs is explained by several factors: (1) They have a high affinity for the water–ice front (liquid–solid interface). (2) They have an excellent structural match to the ice crystal, which inhibits the growth of the ice front.<sup>6</sup> As a result of the adsorbed AFPs, a curved water ice front is formed and locally the melting point is depressed, an effect closely related to that of surface curvature upon nucleation (discussed in the coming subsection).

From a thermodynamic perspective, a precise understanding of the mechanism for ice nucleation, i.e., the process initiating ice crystallization and frost formation, is of fundamental importance to the development of effective and sustainable icephobic concepts. In this spirit, we are reviewing, discussing, and proposing anti-icing concepts in the framework of classical nucleation theory.

**2.1. Classical Nucleation Theory.** One of the most common approaches to describe ice nucleation is given by classical nucleation theory (originally derived by Turnbull, Vonnegut, and Fletcher<sup>7</sup>), which has been utilized and further elaborated on by a large number of research groups worldwide. Over the past decade, scientists have shed new light upon the sometimes unexpected and unpredictable behavior of supercooled water droplet freezing on hydrophilic, hydrophobic, and superhydrophobic surfaces varying in surface texture, curvature, and chemical composition.<sup>8–10</sup> The combination of the present nucleation theory and specific thermodynamic properties of confined/interfacial water in contact with the surface was

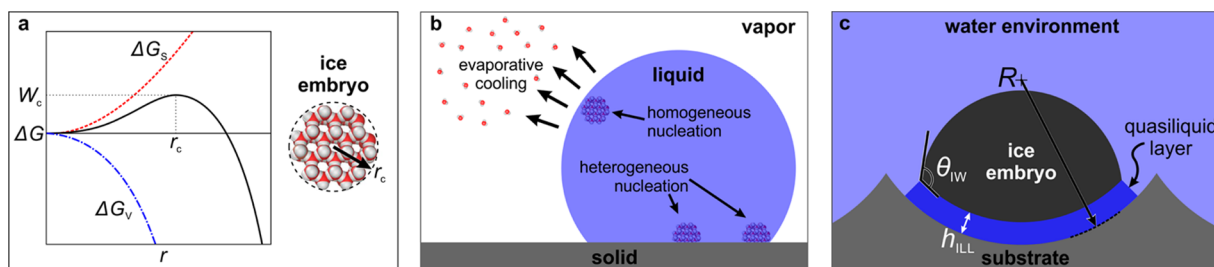


**Figure 2.** Schematics illustrating important aspects of nucleation. (a) Homogeneous nucleation. Plot of  $\Delta G$  vs embryo radius ( $r$ ), showing that beyond a critical value,  $r_c$ , the growth of the ice embryo is energetically favorable (homogeneous nucleation). The inset image is a schematic of an ice embryo of critical size. (b) Nucleation. Schematic depicting the regions within a water droplet where ice can nucleate and potential influences (e.g., evaporation). (c) Effect of curvature. Ice embryo formation on a solid surface with concave surface features that have a radius of curvature  $R$  with  $R \approx r_c$ . A quasi-liquid layer of effective thickness  $h_{ILL}$  ( $h_{ILL} \propto R^{-1}$ ) is depicted and affects the resulting  $\theta_{IW}$  value. Please note that the ice embryos, water molecules, and quasi-liquid layer appear disproportionately to facilitate the aspects of nucleation. The size of an ice embryo is on the order of 1 nm, and the quasi-liquid layer thickness is on the order of a few atomic layers.

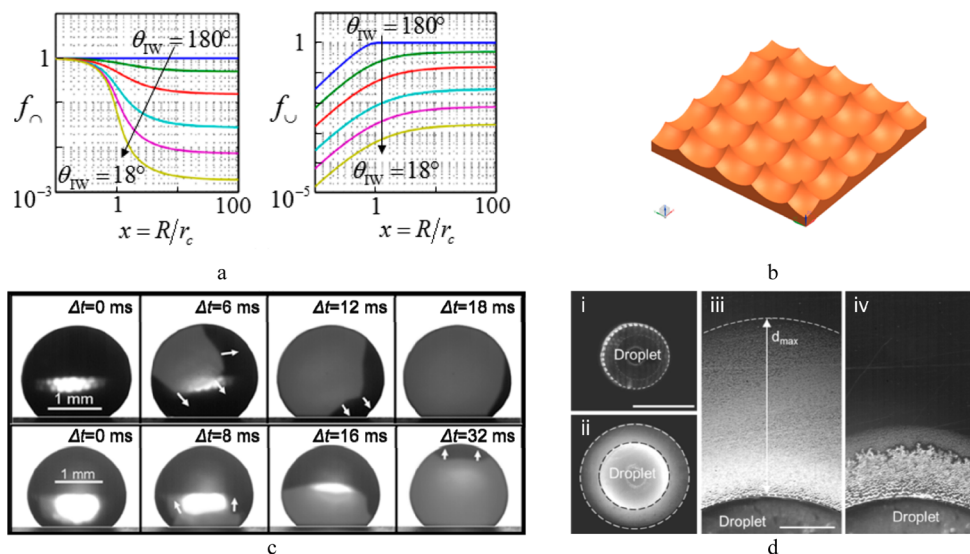


**Figure 3.** Ice nucleation and formation. (a) The geometrical factor  $f$  is plotted against the ratio  $x = R/r_c$  for  $f_c$  (convex roughness) and  $f_u$  (concave roughness) for varying values of  $\theta_{IW}$  ( $180^\circ$ ,  $90^\circ$ ,  $60^\circ$ ,  $36.9^\circ$ ,  $25.8^\circ$ , and  $18.2^\circ$ ; ref 10; reproduced by permission of The Royal Society of Chemistry). (b) Hypothetical surface of an array of nanoscale pits with infinitesimal small asperities for extremely low nucleation temperatures (details in the main text). (c) Origin of homogeneous nucleation at the gas–liquid interface followed by ice front propagation in a supercooled sessile droplet (top row), origin of heterogeneous nucleation at the liquid–solid interface followed by ice front propagation in a supercooled sessile droplet (bottom row); ref 9, reproduced by permission of Nature Publishing Group. (d) Top view of (i) a water droplet on a poly(methyl methacrylate) (PMMA) substrate, (ii) a concentric water condensation halo, and (iii, iv) frost formation from a freezing supercooled sessile droplet on a PMMA substrate; ref 27, reproduced by permission of the National Academy of Sciences, USA.

employed in a thermodynamic framework for the rational design of robust icephobic surfaces for long freezing delays.<sup>10</sup> It was also used to predict an ideal icephobic surface texture for extremely low nucleation temperatures (the temperature at which spontaneous freezing takes place).

For a new phase to be initiated and grow, favorable conditions for stable nucleation must be fulfilled, i.e., the free energy barrier for ice embryo formation must be overcome (Figure 2a). To understand the role of ice nucleation in crystallization events, such as the freezing of water droplets in contact with a solid surface, we consider the ice nucleation rate ( $J$ ) for a water droplet on a surface<sup>8,10</sup>

$$J = K \exp\left(\frac{-\Delta G}{k_B T}\right) \quad (1)$$

where  $K$  is a kinetic prefactor representing the attraction (adsorption and integration) of free water molecules to a forming ice embryo,  $\Delta G$  denotes the thermodynamically derived energy barrier for the formation of a critical ice embryo (the minimum stable size a nascent ice crystal needs to be reach to initiate freezing), and  $k_B$  is the Boltzmann constant. As indicated in Figure 2a,  $\Delta G$  can also be seen as the maximum work  $W_c$  (combination of volumetric and surface work) required to form a nucleus of the crystalline phase in the bulk liquid (homogeneous nucleation) or at the interface between the bulk liquid and a solid phase (heterogeneous nucleation). The free energy barrier  $\Delta G$  and factor  $K$  in eq 1 depend strongly on the degree of supercooling of the liquid, which will be further discussed. Clearly, theory and experiment show a strong bearing on temperature for the nucleation rate in homogeneous and heterogeneous nucleation as reported in the literature.<sup>7,8,10</sup>

The kinetic factor,  $K$ , describes the diffusion of water molecules across the water–ice interface of the ice nucleus, including the water molecule number density at the ice nucleus–

water interface and the diffusion activation energy for a water molecule to cross this interface. One can imagine that the diffusivity of water, expressed by the diffusion activation energy in the factor  $K$ , depends not only on temperature, as expressed by the empirical Vogel–Fulcher–Tammann equation,<sup>7</sup> but also on liquid composition, impurities, and thermodynamic boundary conditions. It was demonstrated in numerical simulations by Nistor et al.<sup>11</sup> that water molecules making contact with a concave ice–water interface (not a solid–water interface) are more likely to be aligned with the ice cluster and freeze directly whereas molecules in contact with regions of convex ice–water interfaces tend to move back into the liquid because molecules are unable to migrate into surface pockets.

**2.2. Heterogeneous Nucleation: The Role of Surface Curvature and the Quasi-Liquid Layer.** The change in Gibbs free energy,  $\Delta G$ , which is the thermodynamic energy barrier to the formation of a critical ice embryo, is a function of temperature and ice–water interfacial energy. The classical nucleation theory shows that the free energy barrier for heterogeneous nucleation ( $\Delta G_{het}$ ) is lower than that for homogeneous nucleation ( $\Delta G_{hom}$ ) at a given temperature, and this reduction is usually expressed as a ratio (less than unity),

$$f = \frac{\Delta G_{het}}{\Delta G_{hom}} \quad (2)$$

This ratio ( $f$ ) is a function of the roughness radius of curvature  $R$  (Figure 2c), that is, not simply the RMS roughness,<sup>10</sup> and the ice–water contact angle ( $\theta_{IW}$ ) that forms at the substrate interface. From nucleation theory, we know that at a given temperature an ice nucleus must reach a critical stable radius ( $r_c$ ) for freezing to initiate and propagate (Figure 2a),

$$r_c = \frac{2\gamma_{IW}}{\Delta G_{f,v}} \quad (3)$$

where  $\gamma_{IW}$  denotes the ice–water interfacial energy and  $\Delta G_{fV}$  represents the difference in volumetric free energy between bulk solid (ice) and bulk liquid, which follows from the Gibbs–Helmholtz equation. For the case in which the surface roughness curvature approaches the critical nucleus radius ( $x = R/r_c \approx 1$ ), the theory reveals a strong bearing of  $R$  on ice nucleation. Figure 3a shows plots of  $f$  for different ice–water contact angle values  $\theta_{IW}$  on surfaces with convex ( $f_{\cap}$ ) and concave ( $f_{\cup}$ ) surface features as a function of  $x$ , where  $x = R/r_c$ . For concave surface features with  $x \approx 1$  and  $\theta_{IW} = 90^\circ$  (nanopits), we see that  $f_{\cup} = 0.2$  and that nucleation should be well enhanced.

Contrary to classical nucleation theory, experiments have shown that the freezing delay time and nucleation temperature are constant for a broad range of RMS roughness values ( $\sim 0.1$  to  $\sim 100$  nm, over 3 orders of magnitude) at approximately  $-25^\circ\text{C}$  ( $r_c = 1.7$  nm).<sup>10</sup> To account for this discrepancy, a hydration layer (i.e., quasi-liquid layer, reduced entropy and enhanced viscosity) was postulated to exist between the forming ice nucleus and the solid surface, therefore affecting  $\theta_{IW}$  and ultimately the nucleation rate of ice.<sup>10,12,13</sup> Although it is reasonable to accept that the change in the properties of this layer is gradual (property gradient between forming ice and solid surface), it is often convenient to employ the quasi-liquid layer presence in theoretical considerations in terms of its average properties taken over an effective thickness. In a recent publication,<sup>14</sup> this hypothesis was also underscored by studying temperature-dependent nucleation rates of ice in contact with hydrophilic and hydrophobic surfaces. The nucleation rate calculations revealed the dominant role of interfacial water on the freezing delay. It is shown in the following section that the presence of a quasi-liquid layer directly influences  $\theta_{IW}$  and thus the freezing delay of the surface.

If we revisit Figure 3a (plot of  $f_{\cup}$ ), we see that when  $x < 10$ , concave nanopits should promote nucleation and therefore dominate the freezing process. Because pits are an unavoidable byproduct of making bumps, one would expect all nanotextured surfaces to enhance nucleation, not suppress it. However, if a quasi-liquid layer forms at the interface between an ice embryo and a solid surface, then this may counteract any ice-nucleation-promoting effects of concave nanopits.<sup>10</sup> This is due to the fact that both the quasi-liquid layer thickness and the effective (through the presence of the quasi-liquid layer)  $\theta_{IW}$  value increase with decreasing  $R$ .<sup>10</sup> Therefore, the nucleation on flatter regions (radii of curvature above  $10r_c$ , where nanopit curvature effects are not important) becomes the dominant mode, resulting in the constancy of the experimentally measured nucleation temperature.<sup>10</sup> Moreover, the presence of confined water in nanopits affects thermodynamic properties of water, e.g., melting point, density, and excess entropy. Hence, because nanopits have not necessarily been shown to enhance nucleation because of the presence of a quasi-liquid layer,<sup>10</sup> they can then be utilized to affect the thermodynamic properties of water (i.e., freezing-point depression), accounting for confinement effects,<sup>10,15</sup> and attempt to maintain a robust liquid layer (confined liquid layer) on the substrate surface.

The discussion above sheds further light on the findings of Jung et al.<sup>8</sup> In contrast to Eberle et al.,<sup>10</sup> it was shown experimentally that surfaces with nanometer-scale roughness close to or even smaller than the critical size of an ice nucleus (e.g.,  $x \leq 1$  in Figure 3a) displayed freezing time delays at least one order of magnitude longer than surfaces with roughness values one or several orders of magnitude larger than the size of the critical nucleus. However, if the relative difference of

experimentally determined freezing delays (a factor of approximately 10 in ref 8) is transformed into a temperature representation, then the change in nucleation temperature turns out to be less than  $1^\circ\text{C}$  (cf. section 2.3). Hence, in the context of nucleation temperature, the effect of surface roughness in this study can be seen as relatively small. We can conclude from the nanopit discussion that surfaces having only a fraction of the area occupied with nanoscale pits below  $10r_c$ , which is the case for most micro- and nanostructured surfaces, will result in a constant nucleation temperature with respect to nanoscale roughness variations.

All of these findings demonstrated the crucial relevance of surface curvature for the physics of icing on surfaces and can be exploited to analyze nucleation in the limit of a hypothetically ideal surface composed of an array of nanoscale pits with infinitesimally small asperities,<sup>10</sup> as shown graphically in Figure 3b. The nucleation temperature of such a hypothetical surface was estimated by Eberle et al.,<sup>10</sup> and it was predicted that the nucleation could be depressed to very low temperatures for very small pit radii of  $r < O(10)$  nm, i.e., high confinement.<sup>10</sup> A more accurate and complex calculation of this kind should involve the effect of the substrate surface atoms on the ice nucleation temperature.<sup>15</sup> Such a surface may also be very efficient against ice adhesion were nucleation barriers to be overcome because an interfacial liquid layer is expected to exist between ice and the substrate, preventing strong substrate–ice bonding (Figure 2c).<sup>16</sup> Such liquid layers, when formed on hygroscopic surfaces, have already demonstrated a substantial reduction in ice–substrate adhesion.<sup>17,18</sup>

**2.3. Freezing Delays.** The effects of substrate wettability and nucleation thermodynamics are intertwined, and studies have reported both delays in ice formation on superhydrophobic<sup>19–21</sup> surfaces as well as the opposite effect.<sup>8,22</sup>

Surface wettability with respect to water can be theoretically linked to surface wettability with respect to ice (ice–water contact angle) by combining the three Young’s-type equations for the contact angles (liquid–vapor–solid, ice–vapor–solid, and ice–liquid–solid), assuming the formation of a spherical segment of an ice nucleus immersed in a supercooled water droplet sitting on an ideally smooth (no surface roughness) solid surface.<sup>8</sup> Accordingly, surface-chemistry-controlled wettability should affect both water and ice–water contact angles and consequently the probability of freezing. This was not confirmed by nucleation experiments, where the ice–water contact angle seemed to be unaffected by surface wettability (liquid–vapor–solid contact angle) for the materials tested.<sup>10</sup> Instead, a clear correlation between the ice–water contact angle variation and quasi-liquid layer formation due to surface-curvature-related water confinement was shown.<sup>10</sup> This has important ramifications for strategies related to surface engineering because the intrinsic wettability modification, which works well for controlling the nucleation behavior in other phase-change processes (e.g., boiling, condensation),<sup>1</sup> may not be a useful tool for controlling the ice nucleation behavior.

Beyond the reported effect of a quasi-liquid layer formation on the freezing delay, Boinovich et al.<sup>23</sup> concluded that for long time scales (of freezing delays), the influence of substrate wettability on the nucleation kinetics is mainly determined by thermodynamically related effects on the energy barrier of embryo formation (exponential factor in eq 1) whereas for short time scales nonstationary effects such as adsorption and the integration of water molecules to a growing and collapsing nucleus (prefactor  $K$  in eq 1) govern the freezing delay. This

finding was compared to the classical heterogeneous nucleation theory assuming the formation of a fully immersed spherically shaped ice nucleus sitting on a substrate.

However, for long time scales, as is the case when dealing with freezing delays on superhydrophobic surfaces, the contact area between the droplet and the solid ( $\phi$ ) has been shown to play an important role in the freezing process. From nucleation theory, a reduced contact area reduces the nucleation rate proportionally by the factor  $\phi = (J_\phi/J)$ . In refs 10 and 23, experiments with varying solid fractions of the contact area with a constant surface chemistry have shown that a reduction in contact area lowers the nucleation temperature and increases the freezing delay times.

Freezing delays are often employed to quantify the icephobic character of a surface.<sup>8,10,20</sup> The rationale for using freezing delays comes from the fact that an icephobic surface should delay the freezing of a supercooled droplet as much as possible. Within the framework of nucleation theory and by employing Poisson statistics, one can express the average freezing delay time required for ice to nucleate in a supercooled droplet as  $\tau_{av} \propto 1/J$  (for constant temperature). Freezing delays are obviously a strong function of temperature because delays are inversely proportional to the nucleation rate from above and eq 1. Their strong relation to temperature is experimentally substantiated,<sup>23</sup> and delays have been shown to increase by up to two orders of magnitude per unit °C.<sup>10</sup> For example, by using a surface at a slightly elevated temperature above its representative ice nucleation temperature, a remarkable average ice nucleation delay of 25 h at  $-21$  °C could be measured.<sup>10</sup> Therefore, one aspect of rational icephobic surface design is to design superhydrophobic surfaces with a low nucleation temperature through controlled nanostructuring guided by thermodynamic principles, where such surfaces should be employed at temperatures slightly above the ice nucleation temperatures for which they are designed.

**2.4. Freezing Locations.** Another important consideration is the thermodynamically favored location for the critical ice nucleus formation (Figure 2b), i.e., water–substrate interface, air–water interface, or air–water–substrate region. Recent experiments and simulations<sup>24,25</sup> show evidence that ice nucleation rates are enhanced near the gas–liquid interface (of droplets), supporting the previous hypothesis of free surface-induced nucleation in supercooled water droplets.<sup>26</sup> For example, experiments by Shaw et al.<sup>25</sup> have shown that for a dry particle, serving as a nucleation site, contacting the free surface of a supercooled water droplet tends to trigger freezing at a higher temperature than in immersion mode where the same particle is fully immersed in the droplet. Moreover, theoretical calculations show the crucial role of free surfaces in the freezing process.<sup>24</sup> Molecular dynamics simulations on supercooled liquid silicon and germanium<sup>24</sup> have demonstrated that the presence of free surfaces, i.e., the gas–liquid interface, may enhance the nucleation rates by several orders of magnitude with respect to those in the bulk liquid, suggesting the transferability of surface-induced nucleation to other tetrahedrally coordinated materials showing a density decrease in solidification such as water.

As shown in Figure 2a, the free energy change for the formation of a critical ice cluster (expressed by free energy barrier  $\Delta G$  in eq 1) is the sum of the ice–liquid interface contribution ( $\Delta G_s$ ) and the volumetric contribution ( $\Delta G_v$ ) of  $\Delta G$ . Because in the case of surface-induced nucleation the forming ice clusters reside in the liquid close to the gas–liquid interface, the variation of the ice–liquid interface contribution of  $\Delta G$  is expected not to

vary significantly compared to bulk-induced nucleation.<sup>24</sup> However,  $\Delta G_v$  is instead decreased (magnitude increases) as compared to the bulk as a result of the free surface energy-induced small lateral pressure ( $p_{lat} < 0$ ) close to the gas–liquid interface, adding a pressure-dependent term  $\delta G_v(p_{lat})$  to the volume free energy change<sup>24</sup>

$$\delta G_v \approx p_{lat}(\rho_L - \rho_I)/\rho_L\rho_I \quad (4)$$

where  $\rho_L$  and  $\rho_I$  are the number densities of the liquid and the forming ice cluster, respectively. It then follows for  $\rho_I < \rho_L$  that the formation of an ice nucleus near the air–liquid interface is more favored by a slightly lowered energy barrier for nucleation, relative to that in the bulk where  $p_{lat} = 0$ . The comparison of stationary and nonstationary nucleation rates of supercooled sessile water droplets also indicate favored nucleation on suspended nanoparticles located at the air–liquid interface with respect to nucleation on the substrate, decorated with the same nanoparticles.<sup>23</sup> The previous discussion provides an indication of how free surfaces, i.e., at the gas–liquid interface, can trigger heterogeneous nucleation due to a small lateral pressure reduction and thus slightly reduced energy barriers for nucleation compared to those for the bulk liquid. This leads to the question of how the enhanced free surface area of water droplets on superhydrophobic surfaces due to surface-texture-related air pockets can have an influence on lowering the energy barrier for nucleation. This may be a very interesting topic for future ice nucleation experiments on superhydrophobic surfaces.

**2.5. Effect of Environmental Conditions.** In the previous discussion, the effects of humidity and gas flow on the nucleation of supercooled water were not taken into account. However, environmental humidity and gas flow, which are naturally present in many icing applications, can fundamentally alter the ice nucleation mechanism, thereby also drastically affecting their icephobic behavior and relevance. It was recently shown<sup>9</sup> that local evaporative cooling of the liquid free surface (Figure 2b) exposed to external gas flow and reduced humidity can render homogeneous nucleation the thermodynamically preferred ice nucleation mechanism instead of commonly expected heterogeneous nucleation on water contacting solids. More specifically, Jung et al.<sup>9</sup> found that under unsaturated gas flow conditions, homogeneous nucleation (from the gas–water droplet interface, first image sequence in Figure 3c) took place. However, under saturated gas-flow conditions heterogeneous nucleation (from the substrate, second image sequence in Figure 3c) was the favored mode, as widely accepted. The change in nucleation mode is explained using nucleation theory combined with the analysis of temperature variation and evaporation of the supercooled droplet under changing environmental conditions.<sup>9</sup> The investigation of the effect of environmental conditions on icing is worthwhile because the mode of nucleation determines the role of the substrate in nucleation events. As an example, consider the homogeneous nucleation case. The nucleation starts from the water–air interface, so the surface no longer solely controls the onset of freezing, and any surface engineering is also restricted by environmental icing conditions.

The formation of a critical nucleus of ice in a supercooled sessile droplet inevitably leads to the explosive release of latent heat upon recalescent freezing, bringing the water from supercooled to equilibrium freezing temperature ( $\sim 0$  °C), resulting in an ice-crystal scaffold (partially solidified liquid).<sup>8</sup> In a second, subsequent freezing stage, the remaining liquid in the interspace of this slushy phase freezes isothermally at a rate that is one to several orders of magnitude slower than the previous one,

which is mainly controlled by the rate at which the heat released during freezing is conducted into the substrate and/or dissipated to the environment.<sup>27</sup> It was demonstrated in ref 27 that the freezing of individual droplets on a relatively low thermal conductivity substrate (polymeric) is associated with a concentric formation and propagation of a condensate halo that ultimately freezes to form an annular frost layer on the substrate adjacent to the droplet (Figure 3d). This process is mainly governed by the low thermal conductivity of the substrate and the degree of supercooling. However, for a substrate with high thermal conductivity (i.e., copper), under an identical relative humidity of 30% and degree of supercooling (15 K), the condensate microdroplets evaporated completely before they could freeze.

This experimental and theoretical investigation of frost formation from supercooled individual droplets clearly indicates a highly effective path of minimization of frost layer formation and propagation for good thermal conductor substrates, unraveling the complex interplay of substrate, droplet, and environment.<sup>27</sup> The presented process<sup>27</sup> involves multiple simultaneous phase transitions, showing ice spreading also by initiating the sequential freezing of neighboring droplets in the form of a domino effect even under undersaturated environmental conditions.<sup>27</sup>

Although frosting can occur from the recalescent freezing of water droplets on low thermal conductivity substrates in an undersaturated environment, it usually forms as a result of a supersaturated environment with respect to ice and/or water. Under these conditions and surface temperatures below 0 °C, frost typically forms either directly from the vapor phase through desublimation or via water vapor condensation, forming supercooled micrometer-sized droplets that eventually freeze through nucleation (condensation freezing).

Frost formation can significantly increase ice adhesion on superhydrophobic surfaces, which poses a major challenge for many icephobicity strategies.<sup>22,28</sup> One of the main issues is that frost nucleation occurs without any spatial preference on superhydrophobic textures. This leads to an increase in the ice–substrate effective contact area, thus leading to an increase in ice adhesion. In an alternative approach to superhydrophobic surfaces, ultrasmooth lubricant-impregnated surfaces (LIS)<sup>29,30</sup> and slippery liquid-infused porous surfaces (SLIPS),<sup>30,31</sup> which exhibit remarkable droplet roll-off properties, have also been studied for antifrosting. After a defrosting cycle (i.e., heating), droplets easily slide off of lubricated surfaces, which keeps the surface free of water and reduces ice formation in the next frosting cycle. In fact, nonwetting surfaces have been utilized to reduce the overall heat consumption during active heating to remove ice as compared to untreated surfaces.<sup>32</sup> LIS and SLIPS may, however, be susceptible to irreversible damage during frost formation, and oil is likely to be depleted from them.<sup>29</sup> Designing icephobic surfaces capable of inhibiting frost formation can therefore be seen as a promising and challenging research path moving forward.

From the preceding discussions on nucleation and the freezing delay, we can highlight the following five aspects: (1) For surface nanoroughness, the nucleation temperature is relatively insensitive to a broad range of nanopit sizes (i.e., radius of curvature). (2) An extraordinary heterogeneous nucleation delay can be theoretically achieved by designing a surface composed of an array of nanoscale pits with infinitesimal small asperities, taking advantage of the presence of the quasi-liquid layer and the freezing-point depression of water.<sup>10,15</sup> (3) Keeping the radius of

curvature of the rough bumps in contact with water smaller than the smallest stable ice nuclei formed increases the energy barrier for ice nucleus formation (retards icing). (4) The nucleation delay can be further increased by minimizing the solid–air fraction of the surface, one instance where icephobicity and superhydrophobicity are linked. (5) Using an icephobic surface that was designed according to the aforementioned principles, in a temperature range above its representative ice nucleation temperature, results in remarkable freezing delay times. With this rational design framework, one can design robust icephobic surfaces for inhibiting heterogeneous nucleation and promoting a freezing delay. From the discussion of freezing locations and the effect of environmental conditions on freezing, we can conclude the following: (1) Theoretical and experimental studies indicate a slightly elevated ice nucleation rate close to the free surface (gas–liquid interface) compared to the bulk liquid (surface induced nucleation). For droplets in contact with a solid surface, this may suggest a favored heterogeneous nucleation site in the water–solid–vapor region (contact line). (2) Under dry conditions with gas flow, ice nucleation may start from the free interface of the droplet (liquid–vapor); therefore, the substrate no longer solely controls the onset of freezing and may limit surface engineering capabilities. (3) Evaporation from a freezing supercooled sessile droplet generates frost halos surrounding it even in a dry environment (undersaturated). The frost halo radius is inversely proportional to the thermal conductivity of the substrate. For low thermal conductivity substrates, this frost formation may initiate freezing to neighboring droplets, resulting in a domino effect, leading to icing propagation. (4) Frost formation can have devastating consequences on icephobic surfaces designed to repel metastable liquid water, e.g., superhydrophobicity. This is due to a lack of control over nucleation processes on the surface. Thus, environmental conditions where frosting is the preferred pathway to ice formation can be seen as an important problem moving forward.

### 3. TRANSPORT: DROPLET MOBILITY

Superhydrophobic surfaces, sometimes referred to as nonwetting surfaces, are characterized by extreme water repellency as well as by enhanced droplet mobility thanks to a combination of high contact angles and low contact angle hysteresis. Superhydrophobicity is achieved when air/gas is trapped at the solid/liquid interface, i.e., between the liquid and the solid substrate, leading to a reduced effective contact between the liquid and the solid substrate. For anti-icing applications focused on preventing the liquid–solid variety of freezing (i.e., metastable liquids), superhydrophobicity can be beneficial by minimizing the contact area between the liquid and the substrate as well as the contact time of an impacting drop,  $t_c$ , allowing surface dewetting before the water can actually freeze and stick to the substrate. Rapid dewetting can be achieved by enhancing the rebound of an impacting drop through an increase in the receding contact angle<sup>33</sup> and/or by shedding of sessile water drops through the minimization of contact angle hysteresis.<sup>9,34</sup> Spontaneous drop removal without external forces was also observed on superhydrophobic surfaces as a result of the jumping motion of the coalesced drops in the dropwise condensation regime.<sup>35</sup> For anti-icing applications, it is essential that superhydrophobic surfaces preserve their nonwetting properties under realistic conditions, at subfreezing temperatures and under dynamic conditions (e.g., repelling a falling water droplet). Particularly, drop impact is a critical aspect for superhydrophobic surfaces because the liquid meniscus may penetrate the surface

texture, displacing the entrapped gas/air. This engenders the loss of superhydrophobicity, causing the drop to stick (be fully or partially impaled) on the surface.

**3.1. Droplet Impalement in Textured Surfaces.** Minimizing the contact time between an impinging droplet and a nonwetting substrate is inherently beneficial to icephobicity because prolonged contact may increase the probability of a nucleation event. The contact time ( $t_c$ ) is proportional to the inertial capillary time scale

$$\tau = (\rho_l D^3 / 8\gamma_{lv})^{0.5} \quad (5)$$

where  $\rho_l$ ,  $\gamma_{lv}$ , and  $D$  are the liquid droplet density, liquid–vapor interfacial tension, and initial drop diameter. This time scale is practically constant for a large range of impacting velocities, but it was shown to be affected by drop break-up<sup>36</sup> and by the value of the receding contact angle.<sup>33</sup> To this end, it is worth noting that phenomena such as liquid penetration into the surface texture and resulting impalement can dramatically affect the solid–liquid contact<sup>37</sup> and cannot be predicted by the simple physics of the above contact time scale.

The droplet impact event is often characterized by the Weber number ( $We$ ), defined as  $We = \rho_l U^2 D / \gamma_{lv}$ , where  $U$  denotes the velocity of impact and is a measure of the ratio between fluid inertia and surface tension forces. The velocity of the water droplet that causes the liquid meniscus to penetrate the surface texture is defined as the critical velocity,  $U_c$ . If the impacting velocity ( $U$ ) is greater than  $U_c$ , then impacting drop does not fully rebound from the surface and remains partially or entirely attached to the surface. This impalement phenomenon is often referred to as the Cassie-to-Wenzel wetting transition and occurs when the impacting pressure of the water droplet overcomes the resistive capillary pressure,  $p_r$ . This pressure is proportional to the surface tension of the water–air interface,  $\gamma_{lv}$ , and the advancing contact angle on the corresponding smooth surface ( $\theta_a$ ).  $p_r$  is also inversely proportional to the characteristic cavity size ( $r$ ) based on the relation<sup>38</sup>

$$p_r \propto \frac{\gamma_{lv} \cos \theta_a}{r_{\text{pore}}} \quad (6)$$

where  $r_{\text{pore}}$  solely depends on the surface topography and can be thought of as an effective pore size. By varying the surface texture, one can increase the capillary pressure to augment the water meniscus impalement stability under impact conditions. It is clear that as the water droplet impact velocity ( $U$ ) increases, so does the associated dynamic pressure ( $p_d \propto \rho_l U^2$ ). However, when  $U = U_c$ ,  $p_d \approx 0.1 p_r$ <sup>39</sup> therefore, the pressure that causes droplet impalement must be of a different origin. Deng et al.<sup>40</sup> proposed that the water hammer pressure ( $p_{\text{wh}}$ ) plays a key role in determining the impalement condition. Because of the water hammer pressure caused by the impacting drop incompressibility, a shock wave is generated at the impact point and propagates at the speed of sound. In their work, Deng et al. proposed an effective water hammer pressure ( $p_{\text{ewh}}$ ) equal to a fraction of  $p_{\text{wh}}$  (prefactor  $\sim 0.2$ ). More recently, Dash et al.<sup>41</sup> found that the prefactor should be modified significantly in accordance with the topography (texture) of the surface and should be  $O(10^{-3})$ . Note that the prefactor of  $p_{\text{wh}}$  is an adjustable parameter that is used to fit the sum of  $p_d$  and  $p_{\text{wh}}$  to the surface capillary pressure  $p_r$  at the critical velocity, i.e., when transition from rebound to stick droplet occurs, and is not derived from physical principles.

The physics behind the impalement mechanism, however, is still not completely understood. In this context, Mandre et al.<sup>42</sup> studied theoretically droplet impact events on a smooth surface, showing that the compressibility of the air layer between the approaching droplet and the substrate is a key feature guiding the first stages of drop impact dynamics. The air layer must be drained from underneath the droplet in order for the liquid to reach the substrate. The compressed air drainage can slow the droplet, leading to regions of high pressure near the impact zone with a characteristic maximum pressure rise ( $p_{\text{max}}$ ). Ultimately, this high pressure deforms the liquid–air interface and forms a dimple. The cusp formation at the dimple periphery increases the liquid pressure (Laplace pressure). What results is a characteristic ring-like meniscus penetration, with a centrally trapped air bubble surrounded by an impaled ring (visualized by X-ray imaging).<sup>43</sup>

Recently, the aforementioned ring-like penetration of the liquid meniscus into the substrate was also reported by Maitra et al.,<sup>37</sup> who systematically studied drop impact behavior on different micro, nano, and micro/nanomultitier surfaces at varying substrate temperatures ( $\sim 20$  to  $-30$  °C) with the aim of understanding the behavior of water droplet impact on severely undercooled surfaces. In this context, the interplay between the intervening air layer and the impact velocity of a water drop is shown in Figure 4. At low impact speed, no penetration occurs

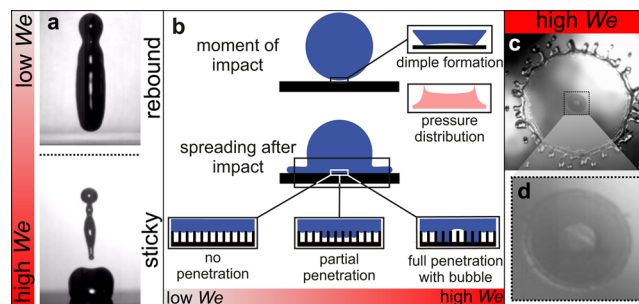


**Figure 4.** (a) Side-view high-speed images showing the receding dynamics of a liquid droplet impacting a superhydrophobic surface for low ( $We \approx 150$ ) and high ( $We \approx 420$ ) Weber numbers; the sticky situation is a result of liquid penetrating the surface texture. (b) Mechanism of liquid meniscus penetration with increasing  $We$ . High values of  $We$  are associated with the formation of a dimple on the impacting droplet and an entrapped air bubble. (c, d) High-speed images showing an impacting droplet ( $U = 3.8 \text{ m s}^{-1}$  and  $We = 461$ ) on a superhydrophobic surface with meniscus penetration (dark region) and the formation of an air bubble (seen in d). Reprinted (adapted) with permission from ref 37. Copyright 2014 American Chemical Society.

and the drop can rebound from the surface. By increasing the impact speed, the partial impalement regime is reached, when liquid starts to penetrate the texture partially upon impact without touching the bottom of the surface. As a result, the drop is still capable of rebounding from the surface, but the contact time increases at low temperature because of viscous effects. For  $U > U_c$ , the liquid meniscus penetrates the surface texture fully and touches the bottom of the surface (full penetration regime), leading to a ring-like region around the impact point. In this area, recoil does not occur and a part of the drop remains attached to the surface.

In particular, it was recently found<sup>37</sup> that a linear trend exists between the characteristic maximum pressure developed in the air layer,  $p_{\text{max}}$ , as found in ref 42, which rises with impact velocity as  $\propto U^{2.8/9}$ , and surface capillary pressure,  $p_r$ , at the velocity of full

impalement. Interestingly,  $p_{\max}$  depends not only on the liquid properties and impact velocity but also on the surrounding air conditions.<sup>42</sup> Stated succinctly, environmental conditions are important to the impalement process.

To reduce impalement (promote liquid meniscus stability),  $p_r$  should clearly be maximized by optimizing the surface chemistry and surface morphology. The surface chemistry can be modified to maximize the  $\cos \theta_a$  term in eq 6. Given that the most hydrophobic materials we know (including alkyl, alkoxy, and perfluorinated silanes having end groups with gradually decreasing surface energies such as  $-\text{CH}_2$ ,  $-\text{CH}_3$ ,  $-\text{CF}_2$ ,  $-\text{CF}_2\text{H}$ , and  $-\text{CF}_3$ ) would provide maximum contact angles of  $\sim 120^\circ$ , the only remaining parameter that can be tuned is the surface morphology, as expressed by the term  $r_{\text{pore}}$  in eq 6. This term can be defined for the general case as the ratio between the cavity area ( $A_C$ ) and its perimeter ( $L_C$ ). As mentioned above, for well-defined surface geometry (micropillar-based superhydrophobic surface), one can calculate the characteristic pore size as

$$r_{\text{pore}} = \frac{A_C}{L_C} = \frac{a_0(1 - \phi)}{4\phi} \quad (7)$$

where  $a_0$  is the diameter of the micropillar and  $\phi$  is the solid area fraction ( $\phi < 1$ ).

**3.2. Drop Impact under Freezing Conditions.** For droplet impact on substrates that are at low temperatures (substrate temperature down to  $-30^\circ\text{C}$ , liquid droplet under ambient conditions), the impact event can be greatly affected by the viscous dissipation, and therefore the contact time rises accordingly.<sup>37</sup> In the case of no impalement, viscous effects on superhydrophobic surfaces can be smaller than on hydrophilic surfaces.<sup>44</sup> However, because the viscous dissipation, which increases because of a 5-fold increase in water viscosity at  $-30^\circ\text{C}$  compared to room temperature, is proportional to the surface area in contact with the droplet, strong viscous effects can be observed in the case of liquid meniscus partial penetration into the textures. In particular, the penetration occurring near the impact point causes the liquid–solid contact area to increase locally. The viscous dissipation would be identical on surfaces having the same solid–liquid wetting area fraction ( $\phi$ ). For pillared surfaces, by reducing the pillar pitch (center-to-center spacing)—which is representative of surface characteristic cavity size—the capillary pressure would increase, aiding against water meniscus penetration. As the partial impalement decreases, the region of solid–water contact area would be less affected by viscous dissipation.<sup>37</sup> This highlights the importance of controlling the cavity size on the surface to resist droplet impalement at low temperature.

The effect of water viscosity at low temperatures on the receding dynamics of a drop during impact is supported by other researchers.<sup>45</sup> Khedir et al.<sup>45</sup> investigated the water rebound mechanism from a superhydrophobic surface when both the drop and the surface were below the liquid freezing temperature. They reported that for a very low impact speed ( $0.54\text{ m s}^{-1}$ ) no variations in the contact time were observed, confirming that at low impact speed no partial penetration occurs (Figure 4), and the contact time is not affected by viscous effects; however, they reported that viscous effects led to a decrease in the drop restitution coefficient with decreasing temperatures.<sup>45</sup>

Because the actual task of icephobic surfaces is repelling droplets under a metastable liquid condition, the study of the impact behavior of supercooled drops on cold substrates is required. What is truly important from an engineering standpoint

is to know whether a metastable liquid is going to solidify during contact with the solid surface. Mishchenko et al.<sup>46</sup> studied the effect of wettability on the freezing transition of a supercooled water droplet upon impact, identifying a threshold between  $-25$  and  $-30^\circ\text{C}$  for a drop to freeze and adhere to superhydrophobic surfaces. However, the critical role played by environmental conditions may have been overlooked. Tests were performed in dry air at room temperature with a relative humidity of 5%. For an air temperature of  $20^\circ\text{C}$ , the corresponding dew point is  $-21^\circ\text{C}$ , remarkably close to the reported rebound-to-stick transition temperature. A hypothesis that was not considered is that, for surface temperatures lower than the dew point, frost may start to deposit on the surface so that the surface is no longer clean and dry and the ice nucleation sites on the surface cause a change in surface wetting and act as nucleation sites for the drop. Indeed, in a different study Varanasi et al.<sup>22</sup> showed that frost formation on superhydrophobic surfaces can significantly affect their performance. The study showed that ice nucleates over the entire superhydrophobic surface (indiscriminately) and that superhydrophobic surfaces in this case also had significantly higher ice adhesion values than did smooth hydrophobic surfaces.<sup>22</sup> Similar results were also reported by Kulinich et al.,<sup>28</sup> who observed an increase in ice adhesion strength in a humid environment.

Bahadur et al.<sup>47</sup> presented a model for predicting the nucleation time during the retraction phase after drop impact onto a superhydrophobic surface. The underlying idea of the model is that the retraction force, which is a function of the apparent receding contact angle, facilitates drop recoil and thus rebound after the maximum spread is reached. Changes in the receding contact angle, resulting from ice nucleation, reduce the retraction force responsible for dewetting, thus delaying or preventing drop recoil and rebound. Increased viscosity of water at low temperature also opposes drop retraction, slowing down the receding phase of droplet dynamics. The model relies on one empirical parameter, the contact angle of ice on a flat surface in liquid water, i.e., the contact angle formed between the liquid water–ice nuclei interface and the solid substrate. It was found that values that were equal to  $90^\circ$  led to the best fitting of the experimental data.

Recently, we were able to investigate the impact behavior of extremely supercooled drops down to  $-17^\circ\text{C}$  on superhydrophobic surfaces<sup>48</sup> and found that increased viscous effects significantly influence all stages of impact dynamics, including meniscus impalement behavior. In addition to the viscous effects on reducing the maximum spreading and increasing the contact time in the case of partial meniscus penetration, we observed that meniscus penetration upon drop impact occurs with full penetration at the center, instead of ring shape, which is common to room-temperature drop impact. This leads to an unobserved mechanism for superhydrophobicity breakdown. For room-temperature drops, the transition from bouncing to sticky (impaled) behavior occurs sharply under the condition of full texture penetration; differently, under supercooled conditions, the full-penetration velocity threshold was increased markedly (increasing by  $\sim 25\%$  for the tested surface) without bubble entrapment. However, failure to completely dewet as a result of viscous effects can still prohibit complete supercooled drop rebound, even though only partial texture penetration takes place.

**3.3. Role of the Gas Layer: Sublimating Surfaces.** The presence and sustainability of a gas layer between a solid surface and an impacting water droplet play critical roles in realizing dewetting, especially at low temperatures.<sup>37</sup> This was particularly

Table 1. Icephobic Surfaces and Their Associated Advantages and Disadvantages

Icephobic surfaces	Description	Advantages	Disadvantages
Untextured	Surfaces exhibiting relatively high receding contact angles.	Reduce ice adhesion; relatively non-susceptible to damage from shear. Reduce condensation nucleation rate ( <i>i.e.</i> , reduce condensation frosting).	No clear ice nucleation strategy; therefore, ice will form. External forces must be used to remove ice.
Single-tier texture	Nanotexture: Hydrophobic surfaces exhibiting high resistance to drop impalement or promoting quasi-liquid layers/confinement effects	Can resist droplet impalement. Can also promote quasi-liquid layers and confinement effects. Can maintain non-wetting states during condensation.	May have an increased nucleation temperature (compared with multi-tier case).
	Microtexture: Hydrophobic surfaces exhibiting high apparent contact angle values and low liquid adhesion	Low-droplet adhesion, so it can repel supercooled droplets. Lower nucleation temperature due to reduced solid-liquid contact area.	Cannot control condensation; susceptible to flooding. May not reduce ice adhesion, surface is damaged during ice removal.
Multi-tier texture	Hydrophobic surfaces consisting of a combination of macro-, micro-, nano-scale features, with each scale affecting/addressing an important process during transport and phase change.	Microscale texture can reduce droplet adhesion and nucleation temperature by <u>promoting an air layer underneath it.</u> Micro/nanoscale texture can resist droplet impalement during dynamic impact and has a low nucleation temperature. It may also promote <u>spontaneous droplet jumping.</u> Macro/micro/nano-scale texture can resist drop impalement, have a low nucleation temperature, and reduce droplet impact contact time.	Currently, drop impact resistance and contact time reduction applies to speeds $<10 \text{ m s}^{-1}$ . Contact time reduction through macrotexturing only applies to $We < 60$ .

evident in a recent study by Antonini et al.<sup>49</sup> employing a sublimating surface. This study showed that sustaining a vapor layer on a surface can be beneficial in avoiding ice formation even under extreme freezing conditions, down to cryogenic temperatures. When a drop impacts a sublimating substrate such as solid carbon dioxide (commonly known as dry ice), a vapor layer due to substrate sublimation is generated at the solid-liquid interface. This vapor layer carries a double benefit, acting both as an air cushion and as a thermal insulator. It allows the drop to hover over the surface in a contactless manner, rebounding or rolling away before it can freeze, despite the sublimating substrate being at extremely low temperature ( $-79 \text{ }^\circ\text{C}$ ), well below the water freezing point. In the same paper, the same phenomenon of floating drops was also demonstrated, taking advantage of the evaporation of a liquid nitrogen film on the substrate at temperatures of as low as  $-196 \text{ }^\circ\text{C}$ .<sup>49</sup>

**3.4. Superhydrophobic Surfaces: Defrosting.** Superhydrophobic surfaces may also present additional strengths by facilitating the cleaning of frosted surfaces during deicing cycles. Along this line, Boreyko et al.<sup>50</sup> investigated the ability of a surface to restore a superhydrophobic wetting state after condensation freezing occurred on the substrate. Because the condensate drops and ice typically form on the entire surface and not only on the top of surface asperities,<sup>50</sup> one would expect that after deicing the liquid water on the surface would be in the Wenzel wetting state, thus pinned to the surface. However, the authors showed that on a nanostructured superhydrophobic surface, after the ice sheet is partially melted into a mixture of water and ice by heating the surface to above  $0 \text{ }^\circ\text{C}$ , the ice-water slush has good mobility and can dewet the surface spontaneously even at low surface tilt. This ability to dewet during a deicing cycle was attributed to the nanostructuring, on the basis of

previous works such as ref 51, where it was shown that nanoscale roughness minimizes the nucleation density of the condensate relative to the density of surface features, enabling the majority of nucleating condensate to grow over the roughness in the energetically favorable Cassie-Baxter wetting state before coalescing with other drops. However, Jung et al.<sup>9</sup> showed that for shear gas flow under supersaturated conditions, superhydrophobic surfaces containing condensate in their surface texture asperities required relatively high shear gas velocities to cause droplet rolling and removal. Such findings are important in order to understand the freezing behavior of water, specifically on nonwetting surfaces, and to define the limits of functionality and applicability of such surfaces with respect to environmental conditions.

From the previous section on droplet transport, we can make the following conclusions: (1) For droplet impact, minimizing the substrate-supercooled water contact time reduces the probability of droplet freezing. (2) At low temperatures, the viscosity of water is increased and affects the recoil dynamics of droplets impacting surfaces, specifically the substrate-water contact time. This effect becomes dramatic when the impact velocity is sufficient to cause the liquid meniscus to penetrate the surface texture partially. (3) By reducing the gap between surface features toward nanotextured, closed-cell geometries, one can minimize the potential for partial impalement of the water meniscus during drop impact. (4) The performance of superhydrophobic surfaces can be severely degraded in an environment where frost can form, something future icephobic surfaces may need to address. (5) The intervening gas layer between a substrate and an impacting water drop plays a very important role in drop dynamics and whether a drop will impale the surface texture (Cassie-Baxter to Wenzel transitions). To

this end, such gas layers can be readily generated by sublimating surfaces and are capable of shedding droplets even at cryogenic temperatures.

#### 4. SURFACE ENGINEERING CONSIDERATIONS

The preceding sections provide a roadmap for guiding the construction of icephobic surfaces. A significant aspect that should be addressed regarding anti-icing surfaces is the consideration of important issues associated with the stability, mechanical robustness, and scalability of the relevant techniques employed. Specifically, innovative materials developed within a laboratory may lack longevity while being exposed to realistic conditions. Additionally, some anti-icing approaches seem to fail when used in industrial applications, and other techniques are not eligible to be implemented for commercial exploitation because of their fabrication complexity and expense.

**4.1. Fabrication.** Table 1 presents a list of state-of-the-art ice-repellent surfaces, which were guided by the aforementioned theories. Figure 5 presents a categorical description of textured

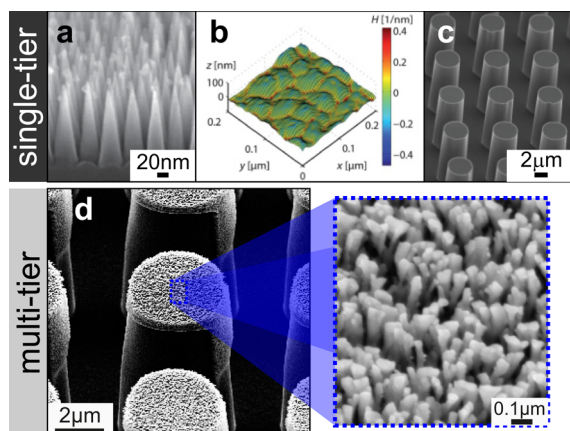


**Figure 5.** Micrographs depicting the relevant length scales and structures utilized in single-tier and multitier structures for icephobicity: (a) nanocones, (b) nanopits, (c) micropillars, and (d) nanotexture/micropillars. The materials are (a) etched silicon nanocones,<sup>66</sup> (b) etched SiO<sub>2</sub> nanopits,<sup>10</sup> (c) etched SiO<sub>2</sub> micropillars,<sup>37</sup> and (d) etched silicon micropillar/nanotexture (nanotexture is shown with the inset image).<sup>37</sup> (a) Reference 66, reproduced by permission of John Wiley and Sons. (b, c) Reference 10, reproduced by permission of The Royal Society of Chemistry. (d) Reprinted (adapted) with permission from ref 37. Copyright 2014 American Chemical Society.

surfaces: single-tier texture (top) and multitier texture (bottom). It also presents a series of images for the nanostructures utilized to enhance a specific aspect of ice repellency: (1) drop impalement resistance and (2) quasi-liquid layer formation. The structures can be pores, cones, pillars, wires, pits, and so forth. For nanopore production, anodization techniques are now capable of producing high-aspect-ratio (>1000) structures on metallic substrates by similar techniques already used in industry for the high-speed production of mechanically robust coatings (i.e., hard anodization).<sup>52</sup> Similar structures have already demonstrated drop impalement resistance; however, the performance may not be sufficient for more intense anti-icing applications.<sup>40</sup> Because metallic surfaces (and their oxides) are natively hydrophilic, hydrophobic thin-film uniform coating treatments are necessary. The durability of such films is an important consideration for long-term performance because degradation leads to the loss of the icephobic property.<sup>53,54</sup> The

long-term stability of thin hydrophobic coating treatments is a problem other multiphase mass-transfer applications have had long-standing issues with, which has limited their industrial use (e.g., condensation).<sup>55,56</sup> Durable multitier superhydrophobic surfaces, either polymeric or metallic-based, are now capable of being generated by single (or few)-step, large-area techniques; however, for icephobic applications, such surfaces suffer from problems similar to those mentioned above.<sup>57–61</sup> Whereas strategies and design exist for the construction of icephobic surfaces and much progress has been made on scalable techniques for the generation of said surfaces, the icephobic performance is still not at a level that is acceptable for many desired applications (cf. section 4.2).<sup>62</sup>

**4.2. Durability (Utility).** Various criteria have been set to evaluate the performance of materials and demonstrate their anti-icing functionality. Ice nucleation delay, ice adhesion, and drop mobility are the most common features that qualify the icephobic behavior of surfaces. All of these aforementioned criteria are necessary to integrate with the practical application-oriented issues mentioned previously. In this section, prospective anti-icing strategies will be presented and their sustainability toward real applications will be highlighted. Table 2 also presents some of the best achievements in anti-icing surface technologies. We will refer to these throughout the following section.

The discussion in section 2 emphasized the need for a rational approach and design of surfaces based on thermodynamics principles and controlled surface structuring to avoid ice formation for a wide range of temperatures. Utilizing this approach, Eberle et al.<sup>10</sup> reported that for a rationally structured icephobic surface a very large freezing delay (as large as ~25 h at -21 °C) can be achieved.

For practical applications, such surfaces should be able to withstand realistic conditions, e.g., prolonged exposure to freezing rain, abrasion, and so forth. Boinovich et al.<sup>53</sup> reported a highly durable, stainless steel-based superhydrophobic surface capable of demonstrating freezing delay capabilities even under prolonged exposure to freezing rain conditions. Also, for the case where icing did occur, the coating was able to maintain its nonwetting property after deicing. Furthermore, the coating demonstrated the ability to retain its nonwetting property even after 100 icing/deicing cycles. Although the icing/deicing test is not relevant for ice nucleation delay tests, it does assess the chemical stability (i.e., tendency to resist hydrolysis) and mechanical durability (due to thermal fluctuations and volume expansion associated with phase transitions); therefore, such a surface can be considered to be well performing from an anti-icing application perspective.

It is clear that the design requirement of an icephobic surface exhibiting a long ice nucleation delay must be complemented by the requirement of mechanical and chemical robustness and stability. For a much more extensive discussion of the effect of repeat icing/deicing cycles on icephobic behavior, we refer readers to refs 2 and 3.

Water droplet impact on supercooled superhydrophobic surfaces is the topic of a number of recent studies. As discussed in sections 2 and 3, the contact time of the metastable liquid droplet with a solid substrate ( $t_c$ ) is a crucial parameter governing water droplet freezing. However, there is a theoretical minimum limit to  $t_c$  for bouncing droplets on superhydrophobic surfaces that do not break up or splash.

Bird et al.<sup>36</sup> implemented a strategy that induced droplet break up, under conditions in which it normally would not, by creating macroscale patterns on a superhydrophobic surface (Table 1).

Table 2. Brief Overview of Recent Achievements in Icephobic Performance<sup>a</sup>

property	test	(dimension)	performance	references
ice adhesion	adhesion strength	(kPa)	~60	Subramanyam et al. <sup>71</sup>
			55	Chen et al. <sup>17</sup>
			40	Kulinich et al. <sup>28</sup>
			27	Dou et al. <sup>18</sup>
			15.6	Kim et al. <sup>30</sup>
	icing/deicing cycles	(number of cycles)	100	Boinovich et al. <sup>53</sup>
			80	Chen et al. <sup>17</sup>
ice nucleation delay	nucleation temperature	(°C)	-24	Eberle et al. <sup>10</sup>
	nucleation delay	$\tau_{av}$ (h)	25	Eberle et al. <sup>10</sup>
drop mobility	droplet impact contact time	$t_c \tau^{-1}$	2.6*	Li et al. <sup>63</sup>
			1.4*	Bird et al. <sup>36</sup>
			0.53*	Liu et al. <sup>64</sup>
	droplet impact impalement resistance	$U$ (m s <sup>-1</sup> )	10*	Checco et al. <sup>66</sup>
			4.3*	McCarthy et al. <sup>65</sup>
			2.6 ( $T = -30$ °C)	Maitra et al. <sup>37</sup>
	$We$	826*	McCarthy et al. <sup>65</sup>	
		227 ( $T = -30$ °C)	Maitra et al. <sup>37</sup>	

<sup>a</sup>Asterisks indicate that the test was conducted under ambient conditions. As was noted in the text, the capillary time and Weber number are defined as  $\tau = (\rho_l D^3 / 8\gamma_{lv})^{0.5}$  and  $We = \rho_l U^2 D / \gamma_{lv}$ , respectively.

When the drop impinges on the macroscale ridges, it splits into smaller water fractions, which rebound from the surface in a shorter time as compared to the nonsplitting condition. The result is a 37% reduction in overall droplet–solid contact time (Table 2). Additionally, they showed that the contact time, which was nondimensionalized by the inertial capillary time ( $t_c/\tau$ , eq 5), was 1.4, which at that time was 46% lower than the best reported in the existing literature ( $t_c/\tau = 2.6$ ).<sup>63</sup> Recently, Liu et al.<sup>64</sup> reported a 4-fold reduction in  $t_c$  for the droplet impact on a multitier superhydrophobic surface (macropillars, nanotextured) as compared to conventional rebound on a nanostructured superhydrophobic surface ( $t_c/\tau = 0.53$ ). Their strategy was to convert the droplet kinetic energy into capillary energy stored as a meniscus penetrated the surface texture; if this energy was rectified into vertical motion on a sufficiently fast time scale, so-called pancake bouncing could occur, resulting in a substantial reduction in contact time. In both studies, the maximum droplet impact velocities and Weber numbers utilized were limited to conditions that severely limit their applications:  $U = 1.2$  m s<sup>-1</sup> and  $We = 53$ <sup>36</sup> and 58.5.<sup>64</sup> In the former case, in many applications velocities greater than this  $We$  value are relevant and break up may occur naturally without the need for special surface textures. In the latter case, if impact velocities are increased sufficiently, then full penetration as opposed to partial penetration of the liquid meniscus may occur, resulting in a full loss of droplet mobility (impaled droplet). Therefore, such macroscale texturing approaches are likely to be utilized for niche applications.

Toward the enhancement of impalement resistance, McCarthy et al.<sup>65</sup> fabricated multitier superhydrophobic surfaces that were able to resist droplets impacting at a velocity of 4.3 m s<sup>-1</sup> ( $We = 854$ ). To put that in perspective, a surface with a critical impact velocity of 5 m s<sup>-1</sup> would be able to repel 70–75% of the total rainfall in West Bengal, India, a natural habitat of the superhydrophobic lotus (i.e., lotus effect).<sup>65</sup> By employing nanocones alone, Checco et al.<sup>66</sup> succeeded in reaching even higher impacting velocities without impalement: 10 m s<sup>-1</sup> ( $We = 694$ ). Regarding high-performance surfaces capable of resisting impalement from relatively fast moving droplets (>100 m s<sup>-1</sup>), Mishchenko et al.<sup>46</sup> suggested that by changing the surface

architecture from open- to closed-cell geometries (i.e., honeycomb-like, brick-like structures) the mechanical robustness of the superhydrophobic surface can be enhanced. High-pressure experiments led them to conclude that such geometries should be capable of repelling droplets impacting with velocities of up to 90–135 m s<sup>-1</sup>. However, this hypothesis is yet to be verified experimentally.

It should be noted that the results of the aforementioned studies were restricted to ambient temperature and conditions. To apply these surfaces to real icephobic applications, it is necessary to consider drop impact experiments under realistic icing conditions (i.e., low temperatures of liquids and/or surfaces). Toward this direction, Alizadeh et al. studied droplet impact on surfaces down to -25 °C.<sup>44,67</sup> Similarly, Maitra et al.<sup>37</sup> demonstrated that for a lower substrate temperature such as -30 °C the critical velocity was remarkably 2.6 m s<sup>-1</sup> ( $We = 227$ ).

Another issue that is of importance is the mechanical stability of the surfaces that undergo the process of drop impact (i.e., coating integrity) because the mechanical stability is closely connected to the viability of the surface for real applications. Although such testing is necessary, a limited number of papers investigated the performance of superhydrophobic surfaces after repeated impact events, where a loss of liquid repellency or erosion may occur. Toward this end, Davis et al.<sup>68</sup> exposed a superhydrophobic nanocomposite coating to an air–water spray with varying impinging speeds of 14.5, 4.5, and 3.4 m s<sup>-1</sup> in order to simulate fog impact. They observed that the antiwetting property of the substrate degraded after sufficiently long exposure. In this instance, the wetting property loss was attributed to the penetration of water into the asperities of the sample microstructure. At higher impact speeds, one would expect erosion to become a dominant factor in property loss, and it is clear that more work on erosion and the impact of high-speed fog onto superhydrophobic surfaces is necessary to elucidate the mechanical limits of these surfaces.

Although this article does not address strategies toward reducing ice adhesion, from a durability perspective, especially as it relates to icephobicity, ice removal tests are effective at assessing the coating durability.

Over the past several years, superhydrophobic surfaces were regarded as a prospective strategy for reducing ice adhesion. A model to justify this implementation was presented by Kulinich et al.,<sup>28</sup> according to which water in the Cassie–Baxter state freezes and the entrapped air below the water reduces the contact area between the finally formed ice and the solid. The same researchers showed a mechanism of surface degradation after the icing–deicing cycle exposure due to the roughness of a superhydrophobic surface. After 20 icing/deicing cycles, the ice adhesion strength of ice was enhanced by 3-fold, verifying their surface degradation model. This outcome indicated that the tested superhydrophobic surfaces were not sustainable, effective materials for anti-icing processes and may have limited applications. The capability of superhydrophobic surfaces to reduce ice adhesion was also tested on helicopter blades.<sup>69</sup> A decrease in the adhesion load on superhydrophobic surfaces ranging from 16 to 70% with respect to the baseline metal material was reported. Superhydrophobic surfaces performed the best under rime ice conditions, occurring typically at temperatures lower than  $-10\text{ }^{\circ}\text{C}$ .

In the search of a more prospective strategy for minimizing ice adhesion, the use of lubricated surfaces may hold promise (ice adhesion performance in Table 2). To this end, a water-immiscible organic liquid with low surface tension has been used to impregnate rough solid interfaces (i.e., LIS, SLIPS) for reducing droplet adhesion significantly.<sup>29,70,71</sup> The great advantage of this technique is that the trapped organic liquid acts as a barrier layer that may prevent the penetration of the condensed water (prior to freezing) or the formed ice and reduces ice adhesion. Wilson et al.<sup>31</sup> exposed SLIPS to repeat freeze–thaw cycles and demonstrated that after 150 cycles it performed satisfactorily. In contrast, Rykaczewski et al.<sup>29</sup> observed that LIS was quite unstable, and after a few frosting–defrosting cycles, it lost its self-healing characteristics and was damaged irreversibly. One possible resolution is a honeycomb-like surface texture, proposed by Vogel et al.,<sup>70</sup> which enabled interlocking of the lubricant, improving stability.

In the same direction, Chen et al.<sup>17</sup> and Dou et al.<sup>18</sup> developed a robust anti-icing surface by employing the solid–liquid concept with the water acting as the lubricant. In one technique, a hygroscopic polymer was grafted onto a microporous silicon wafer, enabling the depression of the freezing point of the formed lubricating water layer. In the other, polymers with ionizable pendant groups were employed, which were more advantageous as a result of their substrate independence. In this way, a lubricating water layer was maintained between the ice and the substrate, eliminating the direct contact of ice with the solid interface. This process decreases the ice adhesion significantly in comparison to that of conventional anti-icing surfaces. Its mechanical stability was also verified by measuring the ice adhesion with a number of abrasion cycles, proving its self-healing ability and stability after 80 cycles (Table 2). This technique can provide longer-term solutions to anti-icing applications because the water layer can be replenished by humidity or even melted ice.

The following are the conclusions that can be drawn from the previous section: (1) Although a great deal of drop impact work has been executed, to date no surface has shown the ability to maintain its nonwetting state under conditions that are relevant to aerospace applications ( $\sim 100\text{ m s}^{-1}$ ), and studies of the erosion behavior of such surfaces are lacking. (2) Although certain fabrication methods may be considered to be large-area, many performance issues (drop impalement resistances,

mechanical durability, and chemical stability) need to be addressed before icephobic surfaces will be realized in practice.<sup>62</sup>

(3) Macrotexturing to create favorable fluid transport behavior for reducing the droplet–solid contact time during impact is limited to specific operating conditions ( $We < 60$ ). Under more realistic operating conditions (high  $We$ ), droplet splash or break up occur naturally; therefore, the liquid will be removed quickly irrespective of the surface macrotecture.

## 5. CONCLUSIONS AND PERSPECTIVE

This article presents the logic and challenges associated with the realization of supericephobic surfaces. Depending on the application, the strategies that were reviewed had the goal of never allowing surface ice to form. This was enabled through the enhancement of liquid drop mobility and removal, freezing temperature depression, and freezing delay enhancement; therefore, the emphasis was not on reducing ice adhesion once ice formed on a surface, as was the focus in many other works. It is our opinion that from a fundamental thermofluids standpoint, an optimum icephobic surface should have the following qualities: (1) It should be a surface chemistry/material with a minimum ice nucleation temperature. Such surfaces can be successfully operated even at a few degrees above this temperature, allowing an extended freezing delay time. (2) The surface texture should have multitier structuring, designed also to account for heterogeneous nucleation thermodynamics, to simultaneously reduce and optimize the liquid–solid contact area (lower nucleation temperature) and to enhance the droplet mobility (reduce contact time, avoid impalement) of metastable liquid phases for the corresponding thermophysical properties. Note that the corollary, self-cleaning effect of superhydrophobicity also decreases the presence of ice-nucleation-promoting impurities. (3) Such surfaces should be designed and utilized for the proper environmental conditions (pressure, humidity, etc.). Particularly adverse environment must be targeted with dedicated surface designs.

From a utility standpoint, the aforementioned surfaces must also have a good degree of robustness/durability (mechanical, chemical, etc.) and fabrication scalability (large-area, cost, etc.). These last topics have received less attention in the literature to date, and we deem it necessary that they become a research priority, hand-in-hand with exploring the associated exciting physics of icephobicity and functional surface sculpturing if the findings of the significant research efforts of the community are to be harvested through broadly used applications.

In terms of additional, little explored research directions and the associated physics, we feel that investigating the effect of thermodynamic properties beyond temperature and departing from atmospheric conditions carry both fundamental importance and application relevance (e.g., high/low pressure, velocity, and humidity environments bring into play exciting physics and materials challenges).

### ■ ASSOCIATED CONTENT

#### 📄 Supporting Information

List of variables. This material is available free of charge via the Internet at <http://pubs.acs.org>.

### ■ AUTHOR INFORMATION

#### Corresponding Author

\*E-mail: [dpoulikakos@ethz.ch](mailto:dpoulikakos@ethz.ch).

### Author Contributions

The manuscript was written through the contributions of all authors. All authors have given approval to the final version of the manuscript.

### Notes

The authors declare no competing financial interest.

### Biographies



Photograph of the LTNT team. Pictured left to right: Christo Stamatopoulos, Carlo Antonini, Stefan Jung, Dimos Poulikakos, Patric Eberle, Tanmoy Maitra, and Thomas M. Schutzius.

Thomas M. Schutzius received his Ph.D. in mechanical engineering from the University of Illinois at Chicago in 2013 under the direction of Prof. Constantine Megaridis. During his graduate studies, he was the recipient of the Dean's Scholar Award (fellowship). He currently holds an ETH fellowship at the Swiss Federal Institute of Technology, working as a postdoctoral scholar under the supervision of Prof. Dimos Poulikakos. His major research interests include thermofluids and surface engineering for efficient fluid management and energy applications.

Stefan Jung studied aerospace engineering at the University of Stuttgart, Germany, and the University of Toronto, Canada, and obtained his Master's degree in 2006. He then joined MBDA Systems and Airbus Group in Munich, Germany, as an engineer and research staff member and earned his Ph.D. degree at ETH Zurich in 2012. His main research interests include phase-change problems, omniphobicity, and ice-phobicity. He is currently a postdoctoral researcher at ETH Zurich with Professor Poulikakos.

Tanmoy Maitra is a Ph.D. candidate in the Department of Mechanical and Process Engineering at Swiss Federal Institute of Technology (ETH), Zurich. His research is on understanding the physics of surface/water interaction at low temperature (below the freezing temperature of water) to address surface icing problem. He earned his B.S. in chemistry and chemical engineering from Presidency College, Kolkata, and University of Calcutta, respectively. Thereafter, he carried out his M.S. in the Chemical Engineering Department, Indian Institute of Technology, Kanpur, where he studied the catalytic activity of carbon nanotubes (CNTs) on graphitic content to enhance the electrical conductivity of CNT-polymer composite-based suspended nanowires.

Patric Eberle received his M.Sc. degree in micro- and nanosystems from ETH Zurich in 2010, and he is currently working towards a Ph.D. in the Laboratory of Thermodynamics in Emerging Technologies at ETH Zurich. His research interests are nanostructured surfaces for anti-icing applications and nanofluidic control of nanoparticles, thermodynamic phenomena on the meso-nanoscale, interfacial physics, and nano-optics.

Carlo Antonini received his B.Sc. and M.Sc. degrees in aerospace and aeronautical engineering from Polytechnic University of Milan and his Ph.D. in industrial engineering from University of Bergamo, Italy. He currently holds a Marie Curie Fellowship as a postdoc at ETH Zurich, Switzerland, in the Laboratory of Thermodynamics in Emerging

Technologies. His main research interest is the study of liquid–solid surface interaction for the development of superhydrophobic and icephobic surfaces against icing.

Christos Stamatopoulos received his B.Sc. in mechanical engineering in 2005 and his M.Sc. in environment and development in 2007 from the National Technical University of Athens, Greece. In 2010, he received his Ph.D. from the same institution on the study of fluid dynamics within tubes of complex geometry (blood vessel models). He also conducted research in developing synergistic techniques for measuring temperature and velocity simultaneously in a flow field. Currently, he is a postdoctoral researcher in Professor Poulikakos' group at ETH Zurich. His research focuses on wettability phenomena (superhydrophobicity) and interfacial phase-change processes (condensation, ice nucleation).

Dimos Poulikakos holds the Chair of Thermodynamics at ETH Zurich, where in 1996 he founded the Laboratory of Thermodynamics in Emerging Technologies in the Institute of Energy Technology, which he currently also heads. His research is in the area of interfacial transport phenomena and thermodynamics across scales with a broad palette of related applications and on the development of transformative energy technologies. The focus is on understanding the related physics on the fundamental level, in particular, with respect to phenomena on the micro- and nanoscales, and employing this knowledge for the development of novel technologies in order to advance the state of the art. Specific examples of current research areas are the 3D functional printing of complex liquids and colloids down to nanoparticle resolution, the science-based design of supericephobic and omniphobic surfaces, the chip/transistor-level 3D integrated cooling of electronics, the development of facile methods for the fabrication of plasmonic sunlight absorbers and the development of surface textures for biological applications under realistic fluidic environments. He has received many recognitions for his contributions. Recent ones include the 2009 Nusselt-Reynolds Prize of the World Assembly of Heat Transfer and Thermodynamics conferences (awarded every 4 years), and the 2012 Max Jacob Award, awarded annually and jointly by ASME and AIChE. He received the Dr.h.c. of the National Technical University of Athens in 2006. In 2008, he was elected to the Swiss National Academy of Engineering (SATW), where since 2012 he has served as president of its science board.

### ACKNOWLEDGMENTS

We gratefully acknowledge Dr. Manish K. Tiwari (UCL) for his guiding role at LTNT in many of the works discussed herein and for input on this manuscript. T.M.S. acknowledges the ETH Zurich Postdoctoral Fellowship Program and Marie Curie Actions for People COFUND program (FEL-14 13-1). T.M.S. thanks Dr. Guo Hong (ETH Zurich) for reviewing the manuscript. T.M. acknowledges partial support from the Swiss National Science Foundation (SNF, grant 200021\_135479). C.A. acknowledges funding through a Marie Curie Intra-European Fellowship (ICE<sup>2</sup>, 301174). C.S. acknowledges support from an industrial grant (ABB).

### REFERENCES

- (1) Attinger, D.; Frankiewicz, C.; Betz, A.; Schutzius, T. M.; Ganguly, R.; Das, A.; Kim, C.-J.; Megaridis, C. M. Surface Engineering for Phase Change Heat Transfer: A Review. *MRS Energy Sustain. A Rev. J.* **2014**, DOI: 10.1557/mre.2014.9.
- (2) Lv, J.; Song, Y.; Jiang, L.; Wang, J. Bio-Inspired Strategies for Anti-Icing. *ACS Nano* **2014**, *8*, 3152–3169.
- (3) Boinovich, L. B.; Emelyanenko, A. M. Anti-Icing Potential of Superhydrophobic Coatings. *Mendeleev Commun.* **2013**, *23*, 3–10.

- (4) Raraty, L. E.; Tabor, D. The Adhesion and Strength Properties of Ice. *Proc. R. Soc. A Math. Phys. Eng. Sci.* **1958**, *245*, 184–201.
- (5) Tyshenko, M. G.; Doucet, D.; Davies, P. L.; Walker, V. K. The Antifreeze Potential of the Spruce Budworm Thermal Hysteresis Protein. *Nature* **1997**, *15*, 887–890.
- (6) Liou, Y. C.; Tocilj, A.; Davies, P. L.; Jia, Z. Mimicry of Ice Structure by Surface Hydroxyls and Water of a Beta-Helix Antifreeze Protein. *Nature* **2000**, *406*, 322–324.
- (7) Hobbs, P. V. *Ice Physics*; Clarendon Press: Oxford, 1974.
- (8) Jung, S.; Dorrestijn, M.; Raps, D.; Das, A.; Megaridis, C. M.; Poulidakos, D. Are Superhydrophobic Surfaces Best for Icephobicity? *Langmuir* **2011**, *27*, 3059–3066.
- (9) Jung, S.; Tiwari, M. K.; Doan, N. V.; Poulidakos, D. Mechanism of Supercooled Droplet Freezing on Surfaces. *Nat. Commun.* **2012**, *3*, 615.
- (10) Eberle, P.; Tiwari, M. K.; Maitra, T.; Poulidakos, D. Rational Nanostructuring of Surfaces for Extraordinary Icephobicity. *Nanoscale* **2014**, *6*, 4874–4881.
- (11) Nistor, R. A.; Markland, T. E.; Berne, B. J. Interface-Limited Growth of Heterogeneously Nucleated Ice in Supercooled Water. *J. Phys. Chem. B* **2014**, *118*, 752–760.
- (12) Golecki, I.; Jaccard, C. Intrinsic Surface Disorder in Ice near the Melting Point. *J. Phys. C* **1978**, *11*, 4229–4237.
- (13) Malenkov, G. Liquid Water and Ices: Understanding the Structure and Physical Properties. *J. Phys.: Condens. Matter* **2009**, *21*, 283101.
- (14) Li, K.; Xu, S.; Chen, J.; Zhang, Q.; Zhang, Y.; Cui, D.; Zhou, X.; Wang, J.; Song, Y. Viscosity of Interfacial Water Regulates Ice Nucleation. *Appl. Phys. Lett.* **2014**, *104*, 101605.
- (15) Arcidiacono, S.; Walther, J.; Poulidakos, D.; Passerone, D.; Koumoutsakos, P. Solidification of Gold Nanoparticles in Carbon Nanotubes. *Phys. Rev. Lett.* **2005**, *94*, 105502.
- (16) Chernyy, S.; Järn, M.; Shimizu, K.; Swerin, A.; Pedersen, S. U.; Daasbjerg, K.; Makkonen, L.; Claesson, P.; Iruthayaraj, J. Superhydrophilic Polyelectrolyte Brush Layers with Imparted Anti-Icing Properties: Effect of Counter Ions. *ACS Appl. Mater. Interfaces* **2014**, *6*, 6487–6496.
- (17) Chen, J.; Dou, R.; Cui, D.; Zhang, Q.; Zhang, Y.; Xu, F.; Zhou, X.; Wang, J.; Song, Y.; Jiang, L. Robust Prototypical Anti-Icing Coatings with a Self-Lubricating Liquid Water Layer between Ice and Substrate. *ACS Appl. Mater. Interfaces* **2013**, *5*, 4026–4030.
- (18) Dou, R.; Chen, J.; Zhang, Y.; Wang, X.; Cui, D.; Song, Y.; Jiang, L.; Wang, J. Anti-Icing Coating with an Aqueous Lubricating Layer. *ACS Appl. Mater. Interfaces* **2014**, *6*, 6998–7003.
- (19) He, M.; Wang, J.; Li, H.; Song, Y. Super-Hydrophobic Surfaces to Condensed Micro-Droplets at Temperatures below the Freezing Point Retard Ice/frost Formation. *Soft Matter* **2011**, *7*, 3993–4000.
- (20) Guo, P.; Zheng, Y.; Wen, M.; Song, C.; Lin, Y.; Jiang, L. Icephobic/anti-Icing Properties of Micro/nanostructured Surfaces. *Adv. Mater.* **2012**, *24*, 2642–2648.
- (21) Tourkine, P.; Le Merrer, M.; Quéré, D. Delayed Freezing on Water Repellent Materials. *Langmuir* **2009**, *25*, 7214–7216.
- (22) Varanasi, K. K.; Deng, T.; Smith, J. D.; Hsu, M.; Bhate, N. Frost Formation and Ice Adhesion on Superhydrophobic Surfaces. *Appl. Phys. Lett.* **2010**, *97*, 234102.
- (23) Boinovich, L.; Emelyanenko, A. M.; Korolev, V. V.; Pashinin, A. S. Effect of Wettability on Sessile Drop Freezing: When Superhydrophobicity Stimulates an Extreme Freezing Delay. *Langmuir* **2014**, *30*, 1659–1668.
- (24) Li, T.; Donadio, D.; Ghiringhelli, L. M.; Galli, G. Surface-Induced Crystallization in Supercooled Tetrahedral Liquids. *Nat. Mater.* **2009**, *8*, 726–730.
- (25) Shaw, R. A.; Durant, A. J.; Mi, Y. Heterogeneous Surface Crystallization Observed in Undercooled Water. *J. Phys. Chem. B* **2005**, *9865*–9868.
- (26) Tabazadeh, A.; Djikaev, Y. S.; Reiss, H. Surface Crystallization of Supercooled Water in Clouds. *Proc. Natl. Acad. Sci. U.S.A.* **2002**, *99*, 15873–15878.
- (27) Jung, S.; Tiwari, M. K.; Poulidakos, D. Frost Halos from Supercooled Water Droplets. *Proc. Natl. Acad. Sci. U.S.A.* **2012**, *109*, 16073–16078.
- (28) Kulinich, S. A.; Farhadi, S.; Nose, K.; Du, X. W. Superhydrophobic Surfaces: Are They Really Ice-Repellent? *Langmuir* **2011**, *27*, 25–29.
- (29) Rykaczewski, K.; Anand, S.; Subramanyam, S. B.; Varanasi, K. K. Mechanism of Frost Formation on Lubricant-Impregnated Surfaces. *Langmuir* **2013**, *29*, 5230–5238.
- (30) Kim, P.; Wong, T.-S.; Alvarenga, J.; Kreder, M. J.; Adorno-Martinez, W. E.; Aizenberg, J. Liquid-Infused Nanostructured Surfaces with Extreme Anti-Ice and Anti-Frost Performance. *ACS Nano* **2012**, *6*, 6569–6577.
- (31) Wilson, P. W.; Lu, W.; Xu, H.; Kim, P.; Kreder, M. J.; Alvarenga, J.; Aizenberg, J. Inhibition of Ice Nucleation by Slippery Liquid-Infused Porous Surfaces (SLIPS). *Phys. Chem. Chem. Phys.* **2013**, *15*, 581–585.
- (32) Antonini, C.; Innocenti, M.; Horn, T.; Marengo, M.; Amirfazli, A. Understanding the Effect of Superhydrophobic Coatings on Energy Reduction in Anti-Icing Systems. *Cold Reg. Sci. Technol.* **2011**, *67*, 58–67.
- (33) Antonini, C.; Villa, F.; Bernagozzi, I.; Amirfazli, A.; Marengo, M. Drop Rebound after Impact: The Role of the Receding Contact Angle. *Langmuir* **2013**, *29*, 16045–16050.
- (34) Milne, A. J. B.; Amirfazli, A. Drop Shedding by Shear Flow for Hydrophilic to Superhydrophobic Surfaces. *Langmuir* **2009**, *25*, 14155–14164.
- (35) Boreyko, J.; Chen, C.-H. Self-Propelled Dropwise Condensate on Superhydrophobic Surfaces. *Phys. Rev. Lett.* **2009**, *103*, 184501.
- (36) Bird, J. C.; Dhiman, R.; Kwon, H.-M.; Varanasi, K. K. Reducing the Contact Time of a Bouncing Drop. *Nature* **2013**, *503*, 385–388.
- (37) Maitra, T.; Tiwari, M. K.; Antonini, C.; Schoch, P.; Jung, S.; Eberle, P.; Poulidakos, D. On the Nanoengineering of Superhydrophobic and Impalement Resistant Surface Textures below the Freezing Temperature. *Nano Lett.* **2014**, *14*, 172–182.
- (38) Bartolo, D.; Bouamirrene, F.; Verneuil, É.; Buguin, A.; Silberzan, P.; Moulinet, S. Bouncing or Sticky Droplets: Impalement Transitions on Superhydrophobic Micropatterned Surfaces. *Europhys. Lett.* **2006**, *74*, 299–305.
- (39) Reyssat, M.; Pépin, A.; Marty, F.; Chen, Y.; Quéré, D. Bouncing Transitions on Microtextured Materials. *Europhys. Lett.* **2007**, *74*, 306–312.
- (40) Deng, T.; Varanasi, K. K.; Hsu, M.; Bhate, N.; Keimel, C.; Stein, J.; Blohm, M. Nonwetting of Impinging Droplets on Textured Surfaces. *Appl. Phys. Lett.* **2009**, *94*, 133109.
- (41) Dash, S.; Alt, M. T.; Garimella, S. V. Hybrid Surface Design for Robust Superhydrophobicity. *Langmuir* **2012**, *28*, 9606–9615.
- (42) Mandre, S.; Mani, M.; Brenner, M. P. Precursors to Splashing of Liquid Droplets on a Solid Surface. *Phys. Rev. Lett.* **2009**, *102*, 134502.
- (43) Antonini, C.; Lee, J. B.; Maitra, T.; Irvine, S.; Derome, D.; Tiwari, M. K.; Carmeliet, J.; Poulidakos, D. Unraveling Wetting Transition through Surface Textures with X-Rays: Liquid Meniscus Penetration Phenomena. *Sci. Rep.* **2014**, *4*, 4055.
- (44) Alizadeh, A.; Bahadur, V.; Zhong, S.; Shang, W.; Li, R.; Ruud, J.; Yamada, M.; Ge, L.; Dhinojwala, A.; Sohal, M. Temperature Dependent Droplet Impact Dynamics on Flat and Textured Surfaces. *Appl. Phys. Lett.* **2012**, *100*, 111601.
- (45) Khedir, K. R.; Kannarpady, G. K.; Ishihara, H.; Woo, J.; Asar, M. P.; Ryerson, C.; Biris, A. S. Temperature-Dependent Bouncing of Supercooled Water on Teflon-Coated Superhydrophobic Tungsten Nanorods. *Appl. Surf. Sci.* **2013**, *279*, 76–84.
- (46) Mishchenko, L.; Hatton, B.; Bahadur, V.; Taylor, J. A.; Krupenkin, T.; Aizenberg, J. Design of Ice-Free Nanostructured Surfaces Based on Repulsion of Impacting Water Droplets. *ACS Nano* **2010**, *4*, 7699–7707.
- (47) Bahadur, V.; Mishchenko, L.; Hatton, B.; Taylor, J. A.; Aizenberg, J.; Krupenkin, T. Predictive Model for Ice Formation on Superhydrophobic Surfaces. *Langmuir* **2011**, *27*, 14143–14150.
- (48) Maitra, T.; Antonini, C.; Tiwari, M. K.; Mularczyk, A.; Imeri, Z.; Schoch, P.; Poulidakos, D. On Supercooled Water Drops Impacting on Superhydrophobic Textures. *Langmuir* **2014**, *30*, 10855–10861.

- (49) Antonini, C.; Bernagozzi, I.; Jung, S.; Poulikakos, D.; Marengo, M. Water Drops Dancing on Ice: How Sublimation Leads to Drop Rebound. *Phys. Rev. Lett.* **2013**, *111*, 014501.
- (50) Boreyko, J. B.; Srijanto, B. R.; Nguyen, T. D.; Vega, C.; Fuentes-Cabrera, M.; Collier, C. P. Dynamic Defrosting on Nanostructured Superhydrophobic Surfaces. *Langmuir* **2013**, *29*, 9516–9524.
- (51) Enright, R.; Miljkovic, N.; Al-Obeidi, A.; Thompson, C. V.; Wang, E. N. Condensation on Superhydrophobic Surfaces: The Role of Local Energy Barriers and Structure Length Scale. *Langmuir* **2012**, *28*, 14424–14432.
- (52) Lee, W.; Ji, R.; Gösele, U.; Nielsch, K. Fast Fabrication of Long-Range Ordered Porous Alumina Membranes by Hard Anodization. *Nat. Mater.* **2006**, *5*, 741–747.
- (53) Boinovich, L. B.; Emelyanenko, A. M.; Ivanov, V. K.; Pashinin, A. S. Durable Icephobic Coating for Stainless Steel. *ACS Appl. Mater. Interfaces* **2013**, *5*, 2549–2554.
- (54) Mobarakeh, L. F.; Jafari, R.; Farzaneh, M. The Ice Repellency of Plasma Polymerized Hexamethyldisiloxane Coating. *Appl. Surf. Sci.* **2013**, *284*, 459–463.
- (55) Paxson, A. T.; Yagüe, J. L.; Gleason, K. K.; Varanasi, K. K. Stable Dropwise Condensation for Enhancing Heat Transfer via the Initiated Chemical Vapor Deposition (iCVD) of Grafted Polymer Films. *Adv. Mater.* **2014**, *26*, 418–423.
- (56) Enright, R.; Miljkovic, N.; Alvarado, J. L.; Kim, K.; Rose, J. W. Dropwise Condensation on Micro- and Nanostructured Surfaces. *Nanoscale Microscale Thermophys. Eng.* **2014**, *18*, 223–250.
- (57) Tiwari, M. K.; Bayer, I. S.; Jursich, G. M.; Schutzius, T. M.; Megaridis, C. M. Highly Liquid-Repellent, Large-Area, Nanostructured Poly(vinylidene Fluoride)/poly(ethyl 2-cyanoacrylate) Composite Coatings: Particle Filler Effects. *ACS Appl. Mater. Interfaces* **2010**, *2*, 1114–1119.
- (58) Schutzius, T. M.; Bayer, I. S.; Qin, J.; Waldroup, D.; Megaridis, C. M. Water-Based, Nonfluorinated Dispersions for Environmentally Benign, Large-Area, Superhydrophobic Coatings. *ACS Appl. Mater. Interfaces* **2013**, *5*, 13419–13425.
- (59) Maitra, T.; Antonini, C.; Auf der Mauer, M.; Stamatopoulos, C.; Tiwari, M. K.; Poulikakos, D. Hierarchically Nanotextured Surfaces Maintaining Superhydrophobicity under Severely Adverse Conditions. *Nanoscale* **2014**, *6*, 8710–8719.
- (60) Jagdheesh, R.; Pathiraj, B.; Karatay, E.; Römer, G. R. B. E.; Huis in't Veld, A. J. Laser-Induced Nanoscale Superhydrophobic Structures on Metal Surfaces. *Langmuir* **2011**, *27*, 8464–8469.
- (61) Asthana, A.; Maitra, T.; Büchel, R.; Tiwari, M. K.; Poulikakos, D. *ACS Appl. Mater. Interfaces* **2014**, *6* (11), 8859–8867.
- (62) Alizadeh, A.; Bahadur, V.; Kulkarni, A.; Yamada, M.; Ruud, J. A. Hydrophobic Surfaces for Control and Enhancement of Water Phase Transitions. *MRS Bull.* **2013**, *38*, 407–411.
- (63) Li, X.; Ma, X.; Lan, Z. Dynamic Behavior of the Water Droplet Impact on a Textured Hydrophobic/superhydrophobic Surface: The Effect of the Remaining Liquid Film Arising on the Pillars' Tops on the Contact Time. *Langmuir* **2010**, *26*, 4831–4838.
- (64) Liu, Y.; Moevius, L.; Xu, X.; Qian, T.; Yeomans, J. M.; Wang, Z. Pancake Bouncing on Superhydrophobic Surfaces. *Nat. Phys.* **2014**, *10*, 515–519.
- (65) McCarthy, M.; Gerasopoulos, K.; Enright, R.; Culver, J. N.; Ghodssi, R.; Wang, E. N. Biotemplated Hierarchical Surfaces and the Role of Dual Length Scales on the Repellency of Impacting Droplets. *Appl. Phys. Lett.* **2012**, *100*, 263701.
- (66) Checco, A.; Rahman, A.; Black, C. T. Robust Superhydrophobicity in Large-Area Nanostructured Surfaces Defined by Block-Copolymer Self Assembly. *Adv. Mater.* **2014**, *26*, 886–891.
- (67) Alizadeh, A.; Yamada, M.; Li, R.; Shang, W.; Otta, S.; Zhong, S.; Ge, L.; Dhinojwala, A.; Conway, K. R.; Bahadur, V.; et al. Dynamics of Ice Nucleation on Water Repellent Surfaces. *Langmuir* **2012**, *28*, 3180–3186.
- (68) Davis, A.; Yeong, Y. H.; Steele, A.; Loth, E.; Bayer, I. S. Spray Impact Resistance of a Superhydrophobic Nanocomposite Coating. *AIChE J.* **2014**, *60*, 3025–3032.
- (69) Tarquini, S.; Antonini, C.; Amirfazli, A.; Marengo, M.; Palacios, J. Investigation of Ice Shedding Properties of Superhydrophobic Coatings on Helicopter Blades. *Cold Reg. Sci. Technol.* **2014**, *100*, 50–58.
- (70) Vogel, N.; Belisle, R. A.; Hatton, B.; Wong, T.-S.; Aizenberg, J. Transparency and Damage Tolerance of Patternable Omniphobic Lubricated Surfaces Based on Inverse Colloidal Monolayers. *Nat. Commun.* **2013**, *4*, 2167.
- (71) Subramanyam, S. B.; Rykaczewski, K.; Varanasi, K. K. Ice Adhesion on Lubricant-Impregnated Textured Surfaces. *Langmuir* **2013**, *29*, 13414–13418.